SPACE TELESCOPE SCIENCE INSTITUTE
Operated for NASA by AURA

Instrument Science Report WFC3 2007-20

WFC3 TV2 Testing: System Throughput on the UVIS Build 2 Detector

Thomas M. Brown
Oct 11, 2007

ABSTRACT

The UVIS spare detector (UVIS build 2) is currently installed in WFC3 during thermal vaccum ground testing. We have performed testing of the end-to-end system throughput on the UVIS channel, and find that it performs near or better than expectations at most wavelengths. However, the performance in the thermal vacuum environment is lower than that found in the ambient ground testing of this detector earlier this year, for two reasons. First, we find that the long wavelength response of the detector is lower at the detector temperature in thermal vacuum (-78 C, which is close to the on-orbit temperature of -83 C) than it is at the ambient temperature (-54 C). Second, we find that there was non-negligible leak of room light into the optical stimulus fibers when in the ambient test; this leak caused a false enhancement of the throughput at some wavelengths, on the order of several percent. Wrapping of these fibers and operating in the dark thermal vacuum chamber has removed this contamination.

Background

The Wide Field Camera 3 (WFC3) is currently undergoing ground testing under thermal vacuum (TV) conditions. Due to work on the UVIS flight detector (UVIS build 1; UVIS-1), the UVIS spare detector (UVIS build 2; UVIS-2) is currently installed in the instrument. Among the tests performed in TV is a measurement of the end-to-end system throughput (i.e., the throughput of the entire instrument excluding the filter and the HST OTA). These tests are performed at NASA/GSFC using an optical stimulus (called "CASTLE") that can deliver flux-calibrated monochromatic light to the WFC3 focal plane with a variety of source sizes. The end-to-end system throughput tests are performed with a 200 micron fiber, producing a spot approximately

20 pixels across on the WFC3 CCD. This large spot allows the throughput to be measured more accurately, because it averages over pixel-to-pixel variation in response and allows a large number of counts in the measurement (generally >> 10,000 electrons) without approaching the saturation limit of the CCD (80,000 electrons per pixel). The current tests are very similar to the tests performed during the first TV campaign (see Brown & Reid 2005, ISR WFC3 2005-02 for details) and to those performed during the ambient ground tests earlier this year (see Brown 2007, ISR WFC3 2007-07 for details). There are two significant differences between the UVIS-2 tests done in TV this summer and the UVIS-2 tests done in ambient in the spring. First, the detector is now at the operating temperature (-78 C) that is close to the temperature that will be used on orbit (-83 C), instead of the temperature achieved in ambient (-54 C). As noted in Brown (2007), this change in temperature could have a significant effect on the long wavelength throughput, and in fact we have found that to be the case. Second, the ambient tests were subject to light leak in the CASTE source fibers; this leak was not present in the CASTLE flux calibration (which is chopped) but was present in the WFC3 illumination, and it caused an overestimate of the throughput by several percent. In the current TV testing, the fibers have been carefully wrapped to prevent room light from leaking into the fibers (where they lie outside of the chamber), and WFC3 itself is in a dark test chamber.

Each UVIS detector consists of two chips. There are various ways the detectors and their chips can be identified, so I summarize this information here. Confusingly, the FITS files for images obtained on the UVIS channel put chip 2 in extension [SCI,1] and chip 1 in extension [SCI,2]. On UVIS build 1, chip 1 is #178 and chip 2 is #18, where these numbers refer to identification numbers used by the GSFC Detector Characterization Lab (DCL). On UVIS build 2, chip 1 is #50 and chip 2 is #40. These chip identifications have been verified by comparing DCL images of the detector (B. Hill, private comm.) against flat-field images taken during the ambient campaign.

Another factor to keep in mind is the absolute gain. Brown & Reid (2005, ISR WFC3-2005-02) assumed a gain of 1.5 e-/DN when measuring the system throughput of UVIS build 1. Subsequent analysis of the gain (Baggett 2005, ISR WFC3-2005-08) showed that the absolute gain of UVIS build 1 on amps A, B, C, and D, was actually 1.53, 1.52, 1.56, and 1.55 e-/DN, respectively. The system throughput tests for chips 1 and 2 are performed on quadrants read by amps A and C, respectively; these gain values have been assumed for UVIS build 1 in the analysis here (i.e., the chip 1 throughput has been scaled by 1.53/1.5, while the chip 2 throughput has been scaled by 1.56/1.5). Preliminary analysis of the gain values for UVIS build 2, taken during the current TV campaign, are 1.57, 1.54, 1.63, and 1.59 (for amps A, B, C, and D; S. Baggett, private comm.). Those factors have been applied here to the throughputs for UVIS build 2, and they are 1% lower than the values assumed in the analysis of the ambient tests of UVIS build 2 (Brown 2007, ISR WFC3 2007-07).

Yet another factor worth checking is the flat-field, which has a fair amount of structure in the UV (see Bushouse 2005, ISR WFC3 2005-21). Inspecting a UV (F275W) flat field obtained in the current ambient campaign, the detector locations used for the throughput measurements with UVIS build 2 appear to be representative of the detector. Performing the same inspection on a

UV (F336W) flat field obtained during the 2004 TV campaign, the throughput measurements were also done in regions representative of the detector.

Results

The results of the TV tests on UVIS build 2 are given in Table 1 and Figures 1 through 12. Figures 1 and 2 show the absolute throughput of the UVIS channel on each chip. As explained above, the throughputs have been corrected to account for the absolute gain on each amp. The throughputs also include a quantum yield correction. The quantum yield correction results from the fact that in the UV, there is a finite chance of producing two electrons on the CCD for one incoming photon. Without a quantum yield correction, a CCD with high quantum efficiency in the UV could appear to have an unphysically high efficiency exceeding unity. The quantum yield correction at a given wavelength w is w/w_c, where w_c is the critical wavelength, 339.68 nm (there is no correction for $w > w_c$)..

The measurements of the throughput are very repeatable. At each wavelength, a throughput run obtains two throughput measurements, and those agree to much better than 1%, such that the points fall on top of each other in the throughput plots. The throughput over longer timescales is repeatable at the level of a few percent. This can be seen in Figures 3 and 4, which show the scatter in throughput measurements vs. wavelength.

By comparing measurements taken at -78 C and -54 C, we find a significant temperature dependance to the detector efficiency at long wavelengths (Figures 5 and 6), in the sense that the detector is more sensitive at higher temperatures. It is worth noting that we will be operating at -83 C in flight, so if this spare detector is actually flown, the red-end throughput will be slightly lower than reported here at -78 C. There is also a non-negligible dependence on temperature at other wavelengths. This temperature dependence is the primary reason the throughput characterization of this detector has changed since the ambient ground campaign (Brown 2007), but removing light leak from the CASTLE fibers has also resulted in a revision of the throughput downward, by a few percent (Figures 7 and 8).

As with UVIS build 1, the results are close to expectations in the optical (based on component measurements in the lab), but significantly higher in the UV (Figures 9 and 10). This is due to a problem with the DCL measurements of the detector QE in the UV (see Brown & Reid 2005). The measured throughput of the spare detector (UVIS build 2) on chip 1 is similar to that on chip 1 of the flight detector (UVIS build 1; Figure 11). However, on chip 2, the flight detector is clearly superior to the spare detector (Figure 12).

Table 1: Throughput measurements for UVIS build 2

wavelength (nm)	observed chip 1 throughput	expected chip 1 throughput	ratio	observed chip 2 throughput	expected chip 2 throughput	ratio
200	0.099	0.077	1.27	0.102	0.104	0.98
205	0.117	0.091	1.29	0.122	0.120	1.02
210	0.143	0.107	1.34	0.149	0.139	1.07
215	0.175	0.122	1.44	0.181	0.158	1.14
220	0.208	0.138	1.51	0.213	0.180	1.18
225	0.250	0.162	1.54	0.253	0.210	1.20
230	0.297	0.186	1.60	0.296	0.239	1.24
235	0.333	0.212	1.57	0.329	0.271	1.21
240	0.350	0.239	1.46	0.341	0.303	1.13
245	0.352	0.245	1.44	0.341	0.308	1.11
250	0.348	0.249	1.40	0.336	0.311	1.08
255	0.341	0.250	1.37	0.328	0.310	1.06
260	0.329	0.251	1.31	0.313	0.307	1.02
270	0.294	0.248	1.19	0.278	0.296	0.94
280	0.297	0.264	1.13	0.275	0.309	0.89
290	0.319	0.287	1.11	0.295	0.339	0.87
300	0.348	0.304	1.14	0.324	0.361	0.90
320	0.353	0.308	1.14	0.331	0.363	0.91
340	0.367	0.310	1.18	0.344	0.361	0.95
360	0.312	0.280	1.11	0.292	0.320	0.91
380	0.337	0.279	1.21	0.320	0.318	1.01
400	0.370	0.332	1.11	0.357	0.354	1.01
450	0.404	0.383	1.06	0.394	0.392	1.01
500	0.411	0.400	1.03	0.401	0.404	0.99
550	0.423	0.419	1.01	0.417	0.420	0.99
600	0.418	0.429	0.97	0.413	0.428	0.96
650	0.403	0.420	0.96	0.394	0.425	0.93
700	0.372	0.384	0.97	0.364	0.386	0.94
750	0.316	0.331	0.96	0.311	0.330	0.94
800	0.244	0.272	0.90	0.248	0.275	0.90
850	0.196	0.227	0.86	0.196	0.225	0.87
900	0.158	0.192	0.82	0.153	0.185	0.83
950	0.097	0.133	0.73	0.094	0.126	0.75
1000	0.038	0.031	1.25	0.038	0.031	1.21

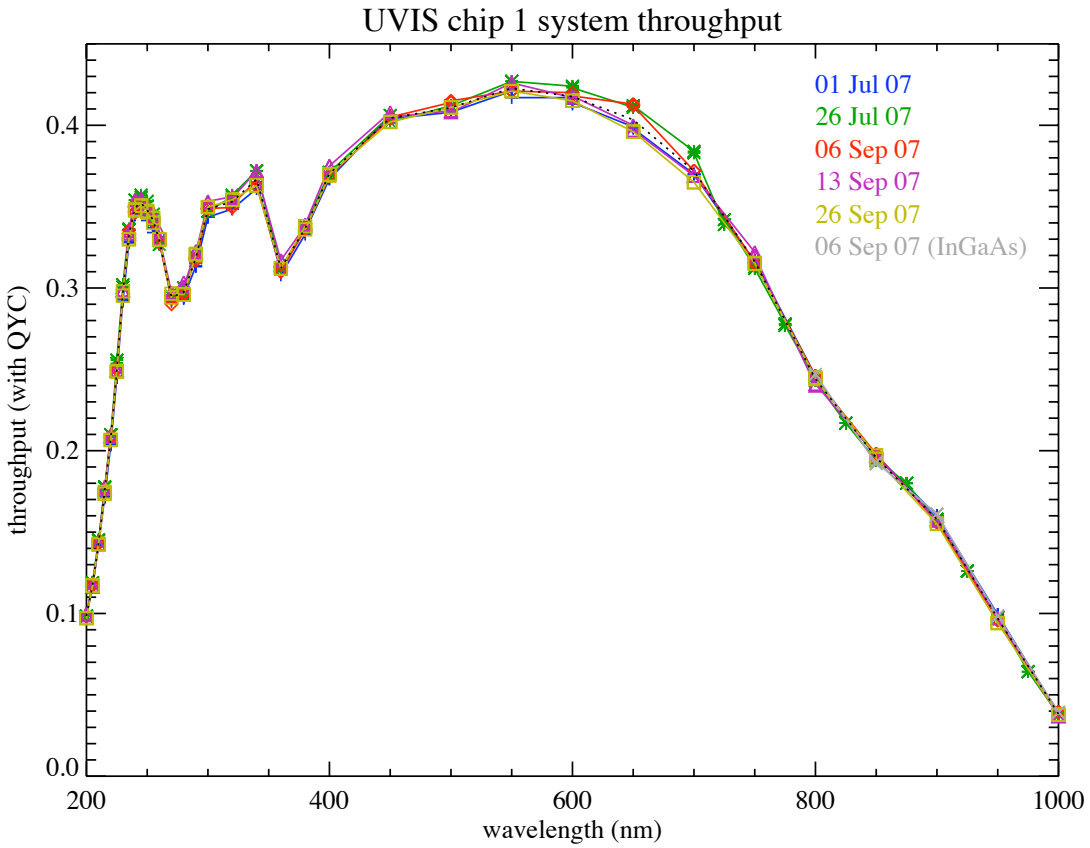

Figure 1: The results of the throughput measurements made on chip 1 at a temperature of -78 C. At each wavelength there are two WFC3 exposures giving nearly identical throughput, so these points fall on top of each other in the plot above. On 26 July (*green points*), a modified version of the test obtained a finer wavelength sampling of throughput measurements longward of 800 nm, and these agree well with an interpolation between the points on the nominal wavelength grid. The CASTLE flux calibration usually uses a photomultiplier tube (PMT) at 600 nm and below, and a Si photodiode at longer wavelengths in the UVIS range. However, on 6 Sep (*grey points*), we measured the throughput at 800 nm and above using the normal WFC3 command script but doing the CASTLE flux calibration on its InGaAs photodiode, which is used for flux calibration above 1000 nm and thus over most of the WFC3 IR channel range. This InGaAs run was done as a sanity check of the IR throughput measurements, and it agrees very well with UVIS throughput measurements made on the nominal Si photodiode.

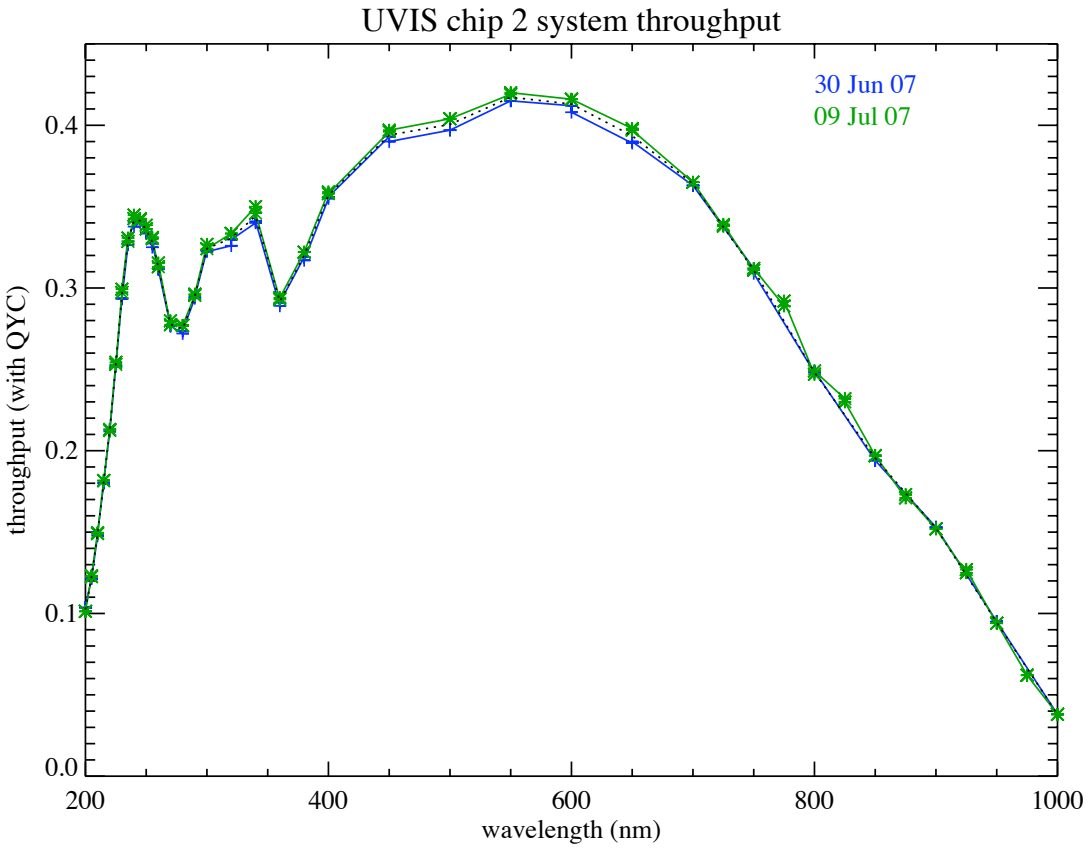

Figure 2: The same as in Figure 1, but for chip 2.

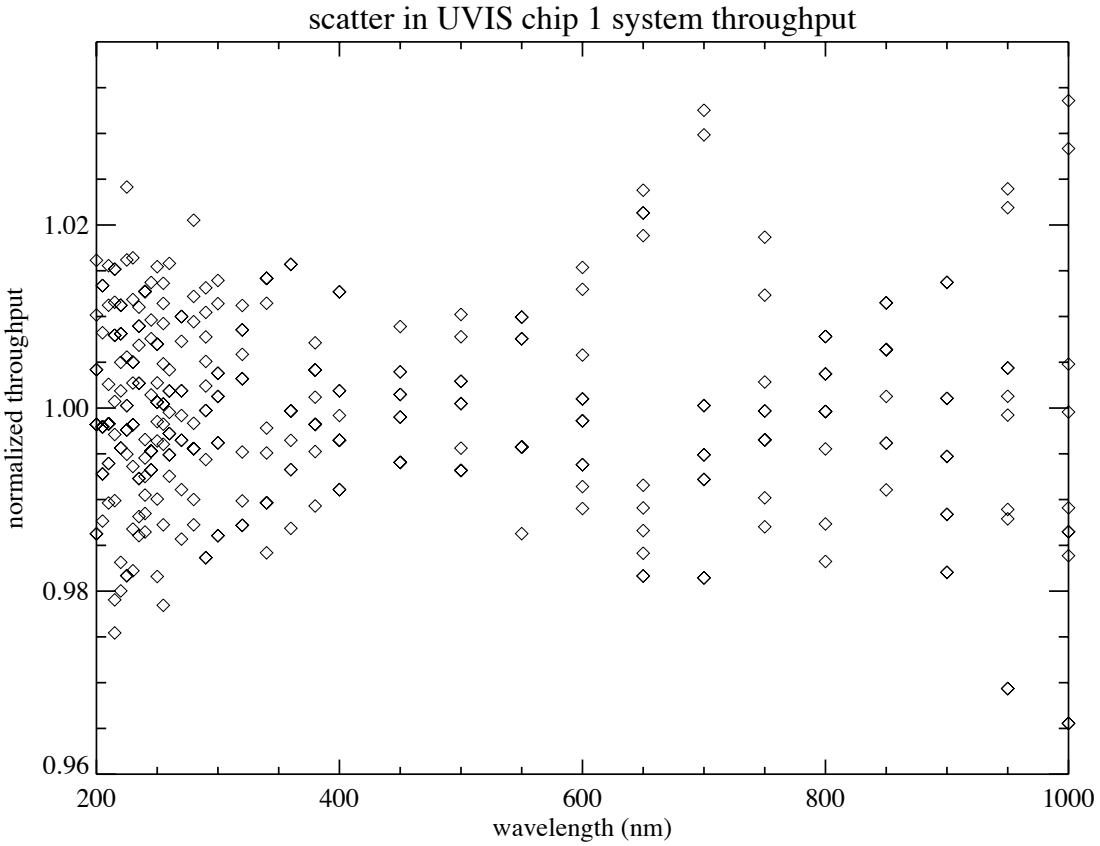

Figure 3: The scatter in throughput measurements vs. wavelength, showing the full set of throughput measurements made at -78 C for each wavelength normalized by the mean throughput at that wavelength. Note that the scatter is from points taken over the course of TV; for each test, there are two throughput measurements taken back-to-back, and those agree so well that they generally fall right on top of each other in the plot above.

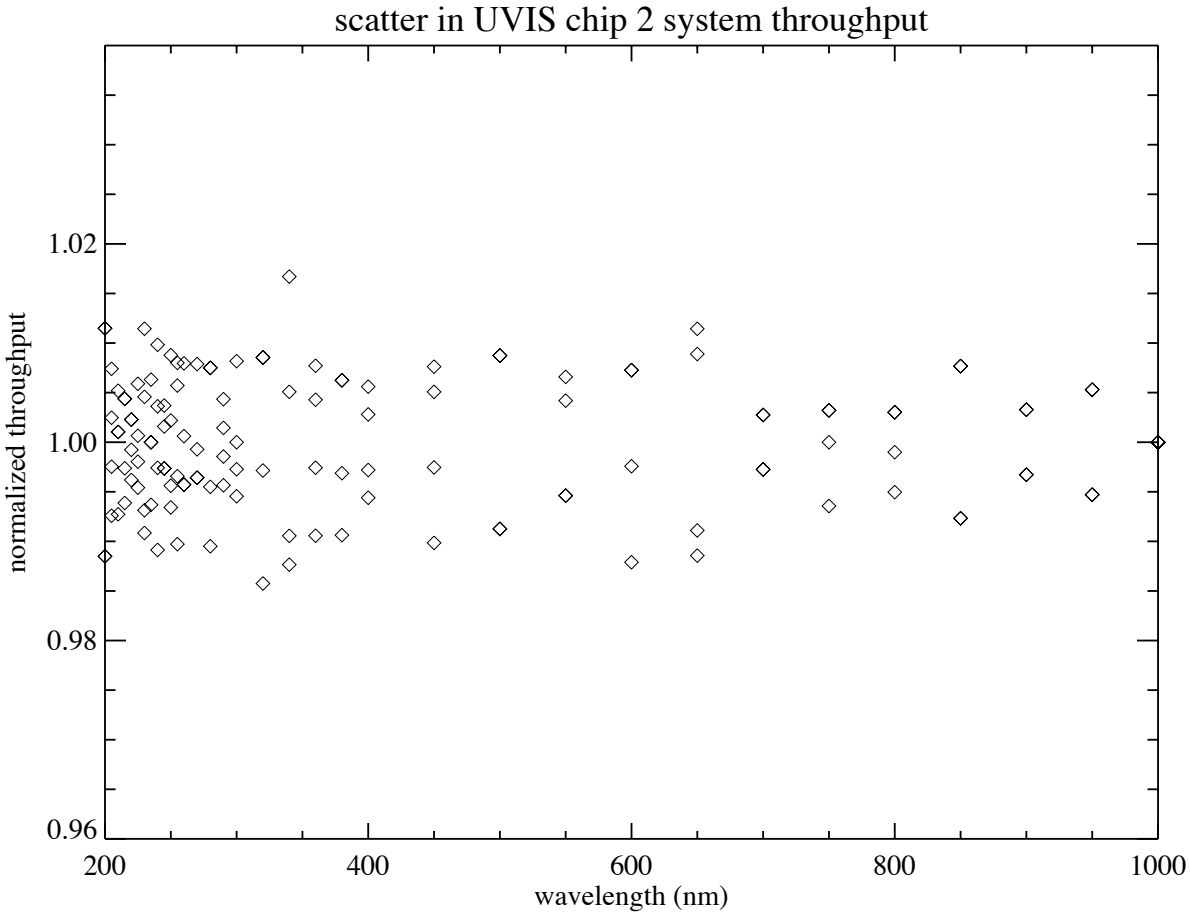

Figure 4: The same as in Figure 3, but for chip 2.

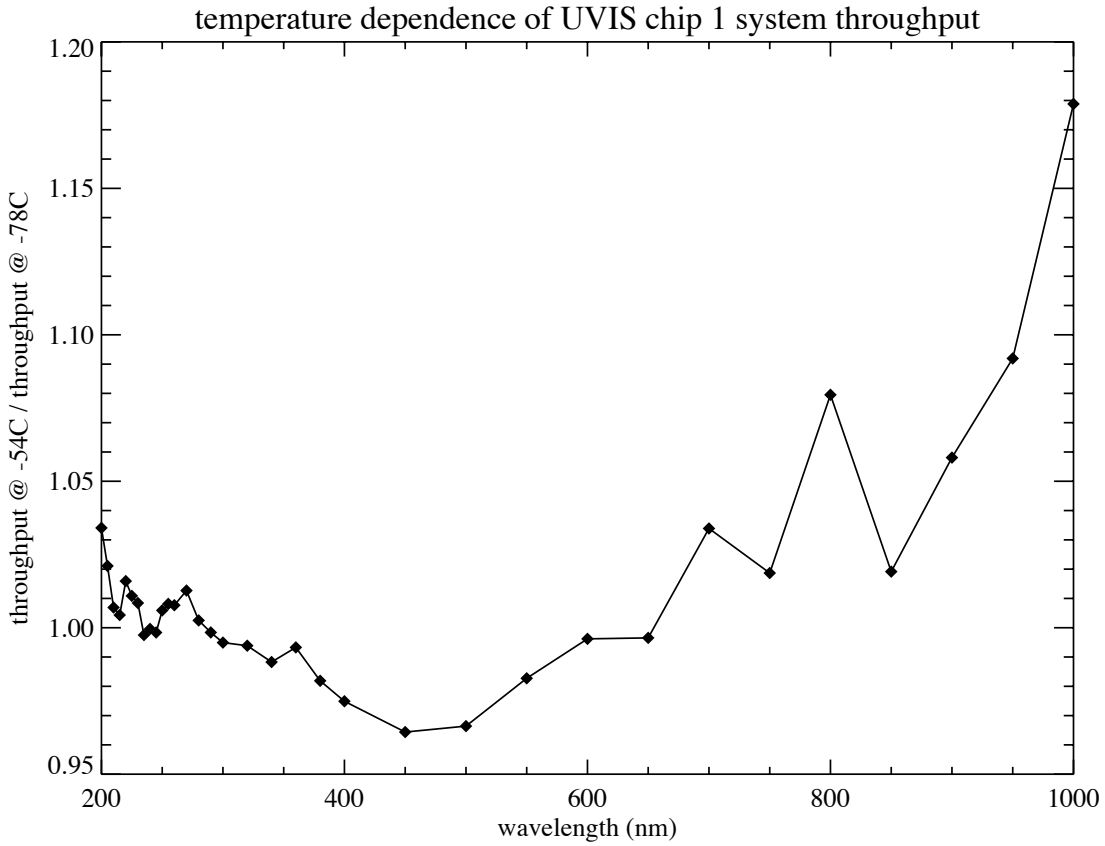

Figure 5: The throughput at -54 C relative to the throughput at -78 C for chip 1. The -78 C throughput is the mean of the 5 nominal throughput runs shown in Figure 1 (i.e., neglecting the InGaAs run). The -54 C throughput comes from a run performed on 15 June. The throughput is significantly higher at long wavelengths when the detector is warmer.

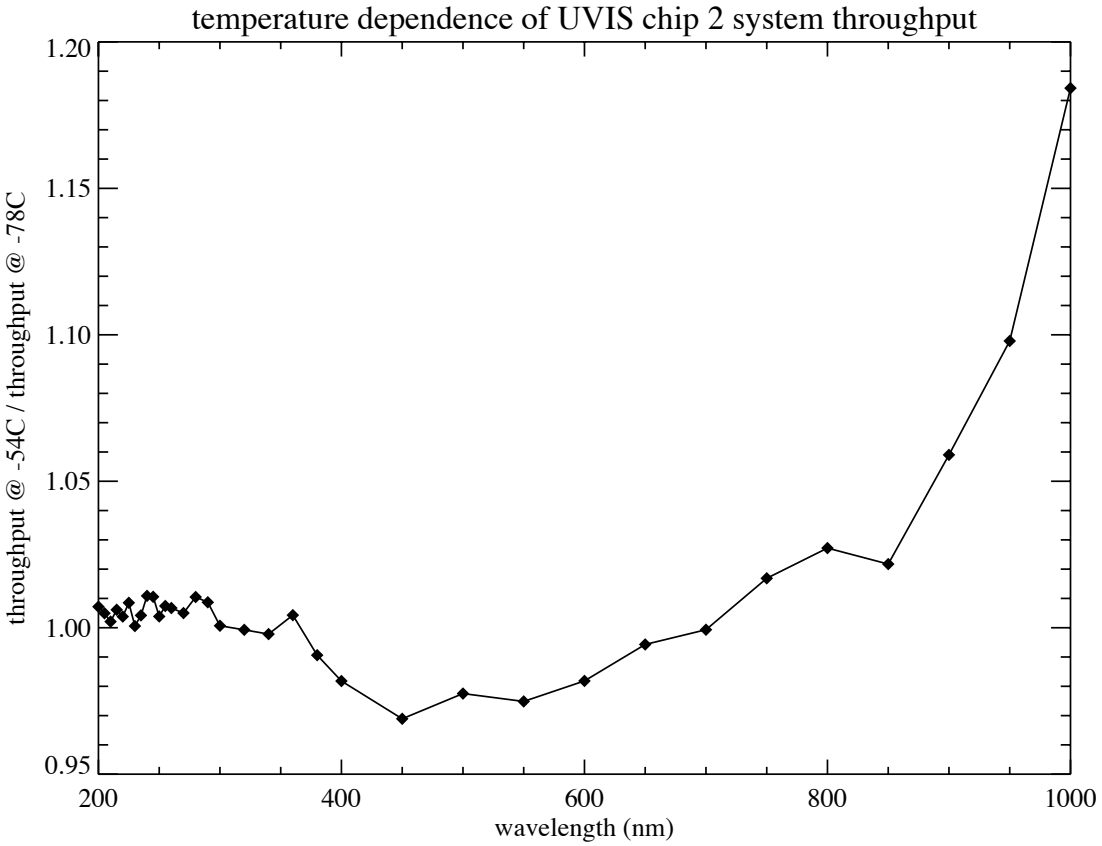

Figure 6: The same as in Figure 5, but for chip 2. The -78 C throughput comes from the mean of the measurements shown in Figure 2. The -54 C throughput comes from runs performed on 15 June and 9 July.

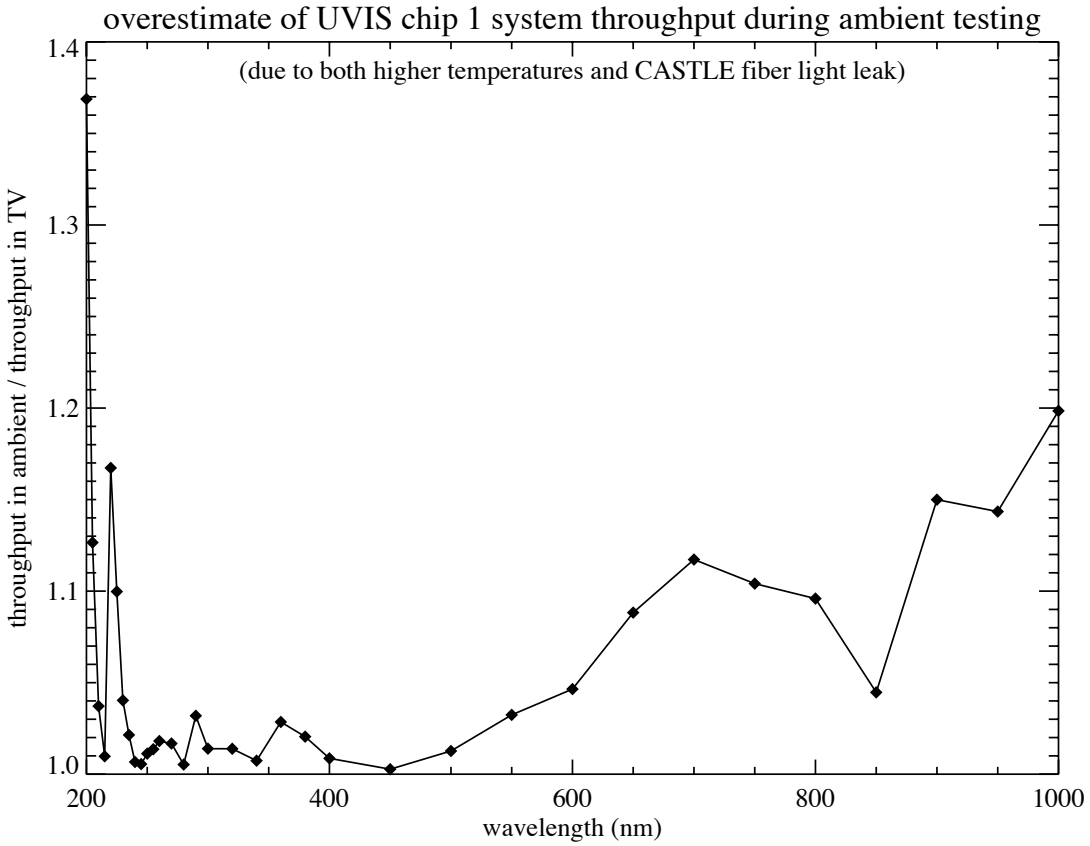

Figure 7: The ratio of the chip 1 throughput measured in the spring ambient campaign (Brown 2007) to the throughput measured at -78 C in the current TV campaign. The throughput measured in ambient was overestimated due to the higher temperature and the CASTLE fiber light leaks.

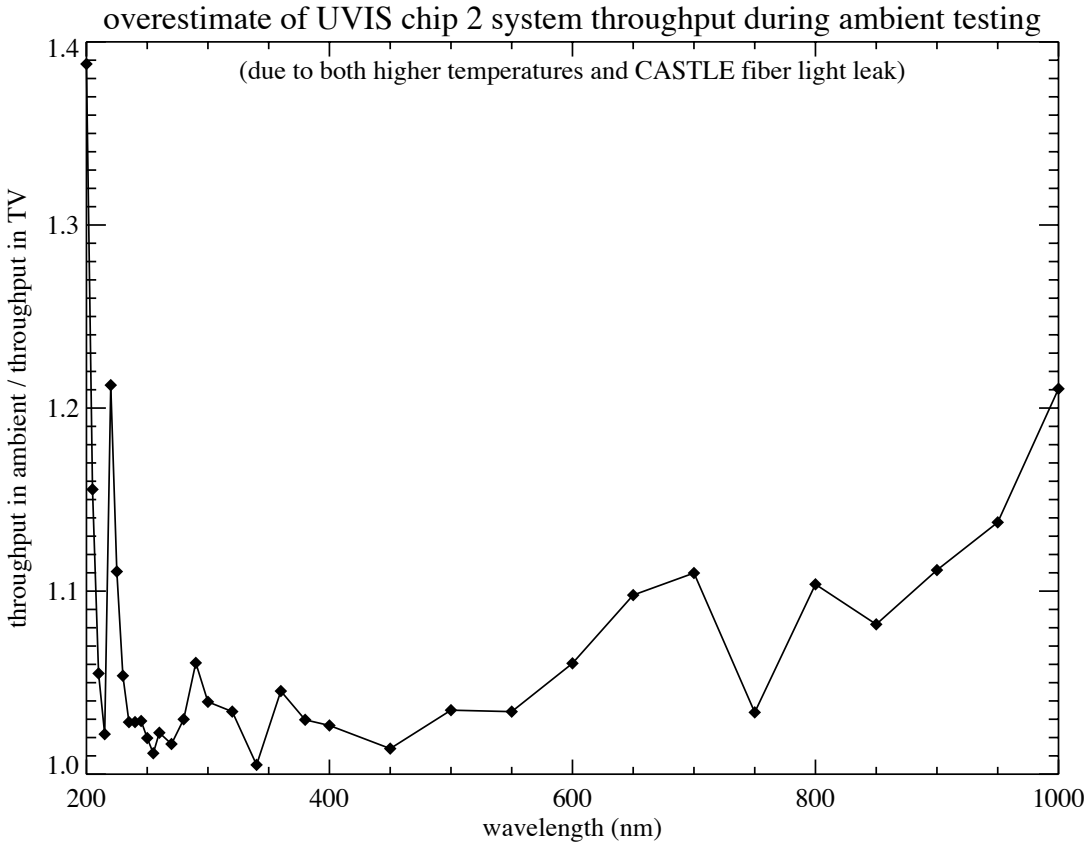

Figure 8: The same as in Figure 7, but for chip 2.

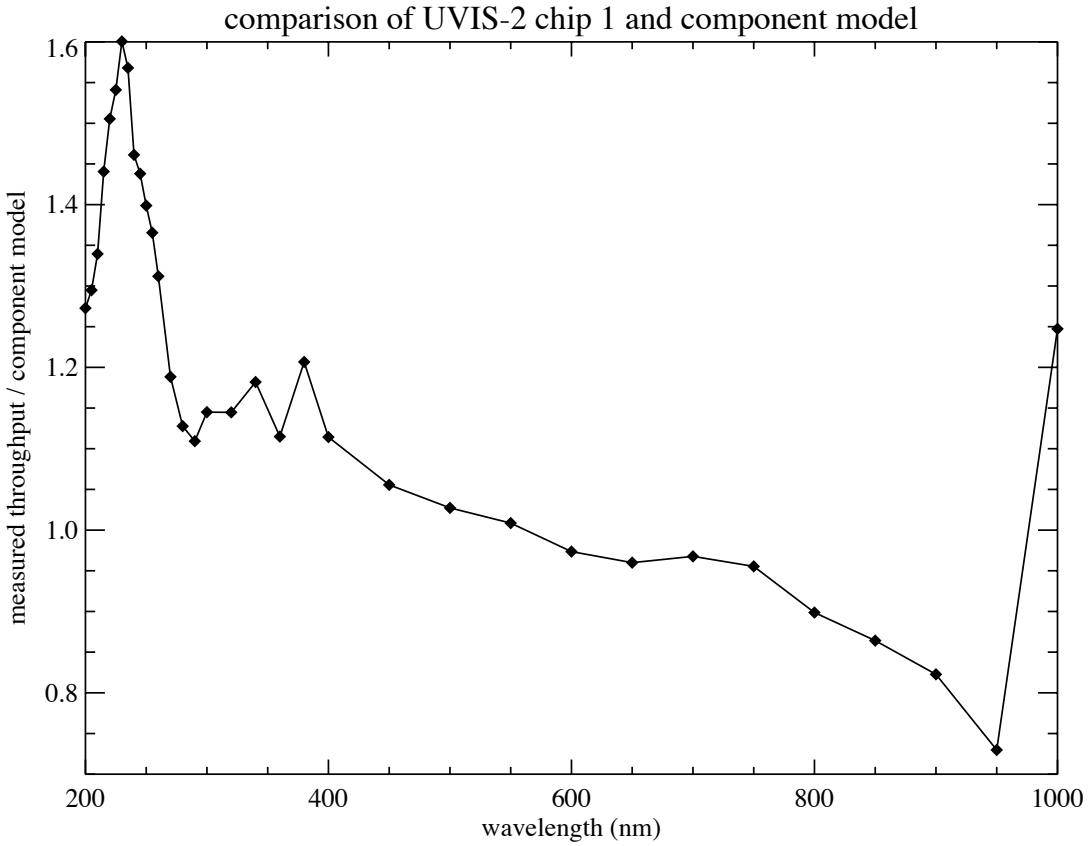

Figure 9: The chip 1 measured throughput relative to the expectation from the component model (i.e., the product of all individual throughputs in the WFC3 system, sans filters).

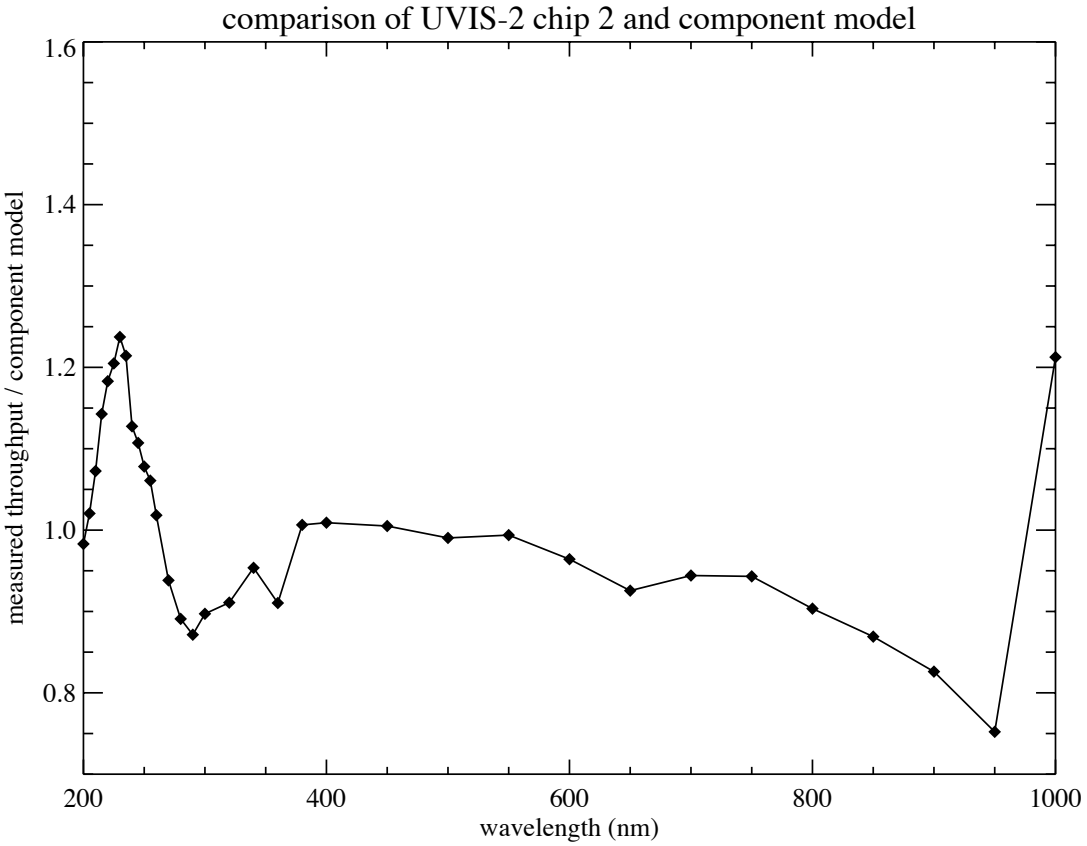

Figure 10: The same as in Figure 9, but for chip 2.

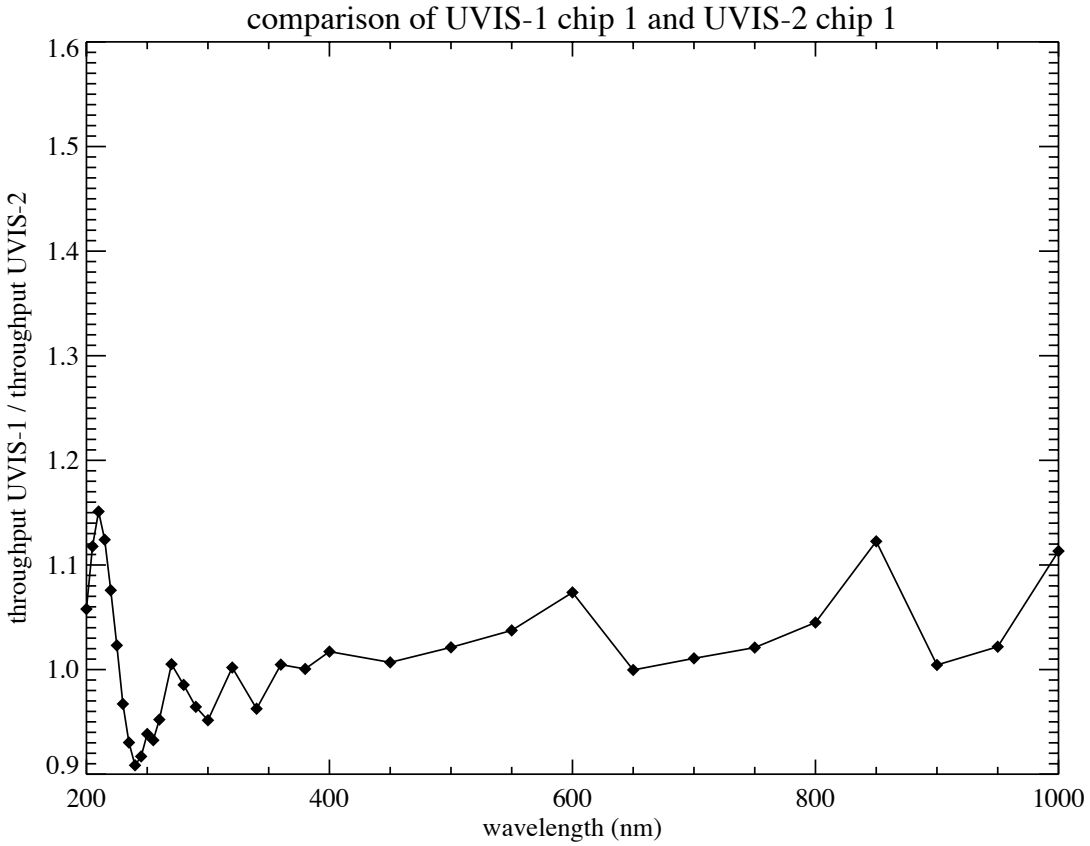

Figure 11: The chip 1 throughput of the flight detector (UVIS build 1; UVIS-1) relative to the chip 1 throughput of the spare detector (UVIS build 2; UVIS-2) currently installed in the instrument during TV tests.

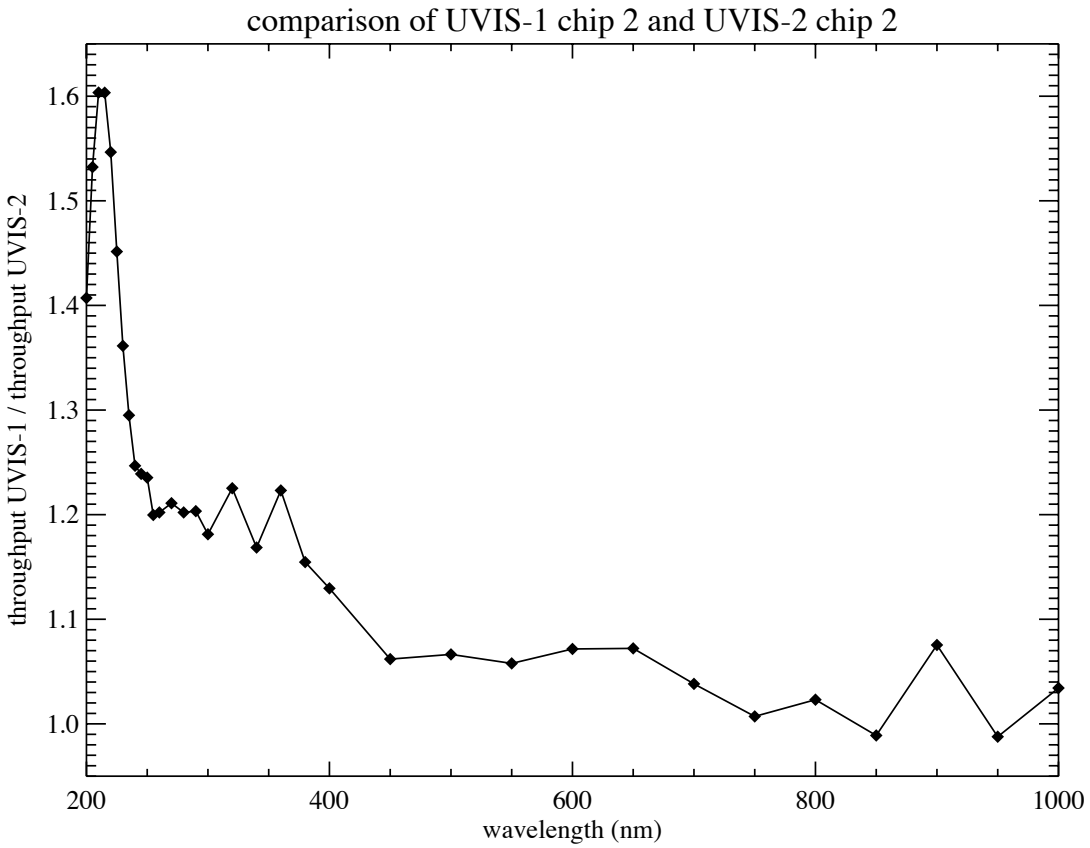

Figure 12: The same as in Figure 11, but for chip 2.